Desalination and Water Treatment
www.deswater.com

doi: 10.5004/dwt.2023.29179

282 (2023) 290–300
January

Research progress on the formation and disappearance of electrocatalytic oxidation active species and the degradation process of azo dyes

Jiping Jia†, Yuke Dai, Yixuan Zhang, Jinyu Gou, Honghua Ge*, Yuzeng Zhao, Xinjing Meng

Shanghai Key Laboratory of Materials Protection and Advanced Materials in Electric Power, Shanghai Engineering Research Center of Energy-Saving in Heat Exchange Systems, Shanghai University of Electric Power, Shanghai 200090, China, Tel.: 008621-60414107; emails: gehonghua@shiep.edu.cn (H. Ge), m17301781770@163.com (J. Jia), yukedai@mail.shiep.edu.cn (Y. Dai), zyx_zhangyixuan@163.com (Y. Zhang), gjy961104@163.com (J. Gou), zhaoyuzeng@shiep.edu.cn (Y. Zhao), mengxinjing@shiep.edu.cn (X. Meng)

Received 5 July 2022; Accepted 2 December 2022

ABSTRACT

Electrocatalytic indirect oxidation is an effective method to efficiently remove refractory organic dyes from water. The production level of active species is a key factor to improve electrocatalytic oxidation. However, side reactions that accompany active species and extremely stable intermediates that may be generated during the degradation process reduce the degradation efficiency. Therefore, understanding the active species of electrocatalytic indirect oxidation and the process of degrading organic matter is very important to improve the degradation efficiency. This paper focuses on the research of the activation mechanism of water and persulfate in electrocatalytic indirect oxidation and the progress of azo dye degradation process. The regularity of specific catalysts to produce active substances and the interaction between active substances were systematically summarized, and the degradation process of azo dyes by active substances was analysed. Some special activation mechanisms that contribute to the practical application of catalysts, as well as organic intermediates that are difficult to remove during degradation, are elucidated. Finally, the prediction methods of activation mechanism and degradation mechanism are prospected.

Keywords: Azo dyes; Electrocatalytic oxidation; Non-free radical process; Radical process; Reaction mechanism

1. Introduction

The pollution of water bodies by various types of refractory organics is a key problem that has been attempted to be solved in water body management in the past 20 y [1]. Although persistent and emerging pollutants are the main focus of attention, the pollution of water bodies by synthetic dyes remains to be resolved due to the mass production of dyes worldwide due to human production needs [2]. According to a research report, the number of dyes in the world exceeds 100,000, and the annual output will exceed 7×10^5 tons [3]. Industries such as textiles, cosmetics, paper, leather, pharmaceuticals, and food packaging generate large volumes of wastewater that are contaminated with high concentrations of dyes and other ingredients [1,2,4,5]. These contaminants include organic and inorganic substances such as softeners, surfactants, inhibitor compounds, chlorine compounds, salts, dyes, total phosphates, perfluorinated compounds, dissolved solids and heavy metal contaminants [2,6–8]. These difficult-to-remove pollutants pose ecological safety and aesthetic concerns to surface water bodies.

Most organic dyes are aromatic compounds with complex structures. Even when exposed to sunlight, microorganisms and oxygen-enriched environments, they still possess

* Corresponding author.
† First-author.

high chemical, biological and photocatalytic stability and resistance to decomposition, and are difficult to remove by general physicochemical or biological methods [9]. At present, the removal of such substances mostly adopts the combination of biological and physicochemical methods or advanced oxidation process (AOP) [1,4]. Biological methods digest organic matter through the metabolic activities of microorganisms, but some toxic substances may inhibit the metabolism of microorganisms and reduce the processing efficiency of microbial systems [10]. Therefore, biological methods need to insert some physicochemical techniques [11–15], resulting in complicated process flow, and these methods and their combined methods still cannot be completely removed [16–18].

Advanced oxidation (AOP) is divided into chemical catalytic oxidation [19], electrocatalytic oxidation [20–28], electro-Fenton oxidation [29], electro-Fenton-like oxidation [30], photocatalytic oxidation [31], acousto-electric oxidation [32] and piezoelectric catalytic oxidation [33]. Different from other treatment methods, AOP can directly or indirectly react organic dyes in multiple steps, and finally produce water, carbon dioxide and some inorganic salts without secondary pollution. It is an effective method to fully mineralize organic dyes.

Electrocatalytic oxidation (EAOP) has been widely used in organic wastewater treatment due to its low energy consumption, high treatment efficiency, no additional intractable waste, and easy improvement of the defects of other AOPs. The search for materials with high catalytic activity has always been an important step to improve the electrocatalytic efficiency, and the improvement of catalytic performance is inseparable from a further in-depth understanding of the activation and production processes of active species [34]. Therefore, a full understanding of the degradation process of intermediate active substances and dyes is an important basis for rationally guiding catalyst synthesis. This paper reviews the effect of electrocatalysis on water and persulfate (PS) activation, summarizes the degradation process of some azo dyes under electrocatalytic direct or indirect oxidation, and provides a link between the active species and the degradation process.

2. Electrocatalytic activation of water and persulfate

The general mechanism of electrocatalytic oxidative degradation of organic dyes is realized by the adsorption and electron transfer of electron donors on the electrocatalyst surface, which requires the electrocatalyst to have a certain number of active sites (oxygen vacancies ($O_v s$) and metal ions with low coordination numbers) [35,36]. According to whether the participating reactants are pollutant molecules, electrocatalytic oxidation can be divided into direct oxidation and indirect oxidation. In direct oxidation, organics act as electron donors directly adsorbed on the active sites on the electrode surface and are oxidized through charge transfer; indirect oxidation utilizes the adsorption and activation of water and supporting electrolytes on active sites by anode to efficiently generate highly electronegative hydroxyl radical ($^{\bullet}OH$), ozone (O_3), active chlorine, singlet oxygen ($^1O_2$), hydrogen radical ($H^{\bullet}$), solvent electron (e^-) and sulphate radical ($SO_4^{\bullet -}$), they can mineralize most organic matter, eventually degrading it into pollution-free H_2O, CO_2, and inorganic salts. Due to the high redox potential (2.5–3.1 eV) of PS, its involvement in indirect electrooxidation is one of the research hotspots in recent years [37]. PS is a general term for peroxymonosulfate (PMS) and peroxydisulfate (PDS). PDS has received extensive attention because of its more practical value. Fig. 1 is a schematic diagram of the mechanism of indirect electrooxidation involving PDS. Due to the synergistic effect of SO_4^- and OH [37,38], the formation mechanism of OH cannot be ignored.

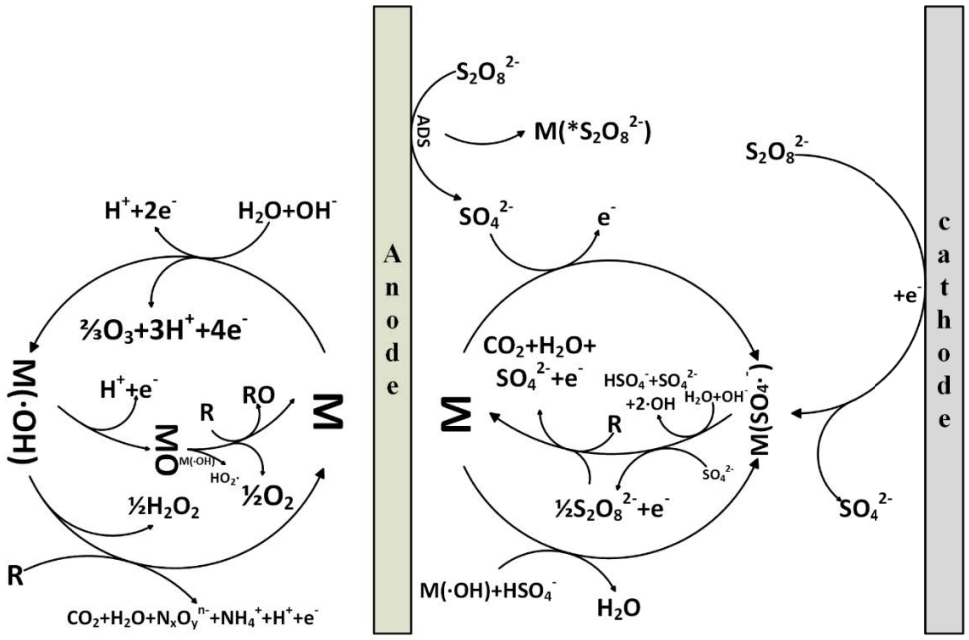

Fig. 1. Mechanism of indirect electro-oxidation of PS and H_2O (M is anode surface, R is organic matter) [3,23,37,39–43].

Fig. 1 clearly shows the source of active substance production and the activation pathway. Because of their high oxygen reduction potential, they can rapidly react with free radicals or other non-pollutant molecules, thus causing unnecessary loss or even failure of active substances.

2.1. Generation and destruction of hydroxyl radicals

The OH generation and destruction mechanism in Fig. 1 can be given by the following reaction equations:

$$H_2O + OH^- + 2M \rightarrow 2M\left(^{\bullet}OH\right) + H^+ + 2e^- \quad (1)$$

$$H_2O + OH^- \rightarrow \frac{2}{3}O_3 + 3H^+ + 4e^- \quad (2)$$

$$M\left(^{\bullet}OH\right) \rightarrow H^+ + e^- + MO \quad (3)$$

$$MO \rightarrow M + \frac{1}{2}O_2 \quad (4)$$

$$2M\left(^{\bullet}OH\right) \rightarrow H_2O_2 + M \quad (5)$$

$$M\left(^{\bullet}OH\right) + MO \rightarrow HO_2^{\bullet} + 2M \quad (6)$$

Since OH is generated by the adsorption and dehydrogenation of water molecules by the anode material [44,45], the adsorption capacity of the material affects the production of OH. The amount of $O_v s$ on the anode surface and the binding energy of OH to the anode surface both affect the adsorption and dissociation of H_2O, and affect oxygen evolution potential (OEP) of the electrode from a thermodynamic point of view [46]. For a specific electrode material, the more $O_v s$, the more places for the adsorption and dissociation of substances, which is conducive to the occurrence of catalytic reactions. Therefore, scholars have developed a variety of preparation methods based on hydrothermal and electrode position methods. By changing the solute of the precursor solution, an electrocatalyst with a special morphology is obtained to achieve the purpose of increasing $O_v s$ [47–49]. Furthermore, the further dehydrogenation of OH leads to the formation of oxides of high oxidation state with lower oxygen reduction potentials on the electrocatalyst surface [Eq. (3)], which adsorb O and OH on the surface of these oxides, which can interact with molecules or free radicals. They collide with each other to form the less oxidizing H_2O_2 and HO_2 [Eqs. (4)–(6)], thereby reducing the yield of OH. In general, the stronger the binding energy of OH to the electrode surface, the lower the OEP, which increases the possibility of side reactions from a thermodynamic point of view [46]. $O_v s$ existing on the surface of different active catalysts has different binding energies of OH, and for the desorption of OH, low binding energy is beneficial to the generation of homogeneous OH [35,50]. Therefore, finding anode materials with more $O_v s$ and optimizing the binding energy of anode materials with OH are the key factors

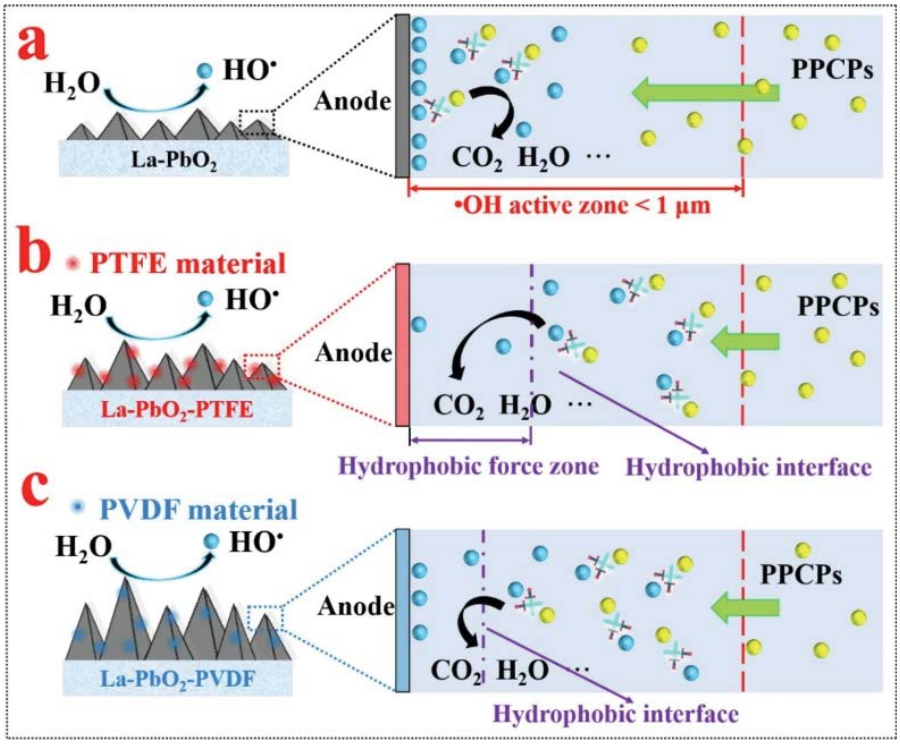

Fig. 2. Schematic diagram of degradation mechanism of PPCPs on the electrodes (Reprinted from Qian et al. [52], License Number: 5437510978948).

to obtain good degradation efficiency. Costentin et al. also analysed the electrocatalytic mechanism from the kinetics of multi-electron, multi-substrate molecular catalysis, and built a model to derive kinetic rate constants from the peak currents and peak potentials of multi-electron and substrate electrocatalytic reactions [51].

The diffusion process of OH in the interface between the catalyst and the bulk solution is often easily overlooked. In order to explore the influence of the interface on the electrocatalytic effect, Qian et al. [52] successfully adjusted the active area of OH (Fig. 2) by hydrophobicizing the surface of the Ti/SnO_2-Sb/La-PbO_2 anode and increased the contact between OH and organic pollutants (Pharmaceuticals and Personal Care Products, PPCPs).

2.2. Active species produced by persulfate

In recent years, some scholars have found that PDS can generate $SO_4^{\bullet-}$ through direct electron transfer on the surface of graphite rods, carbon fibres and Pt cathodes [37]. Furthermore, a non-radical pathway exists for the activation of PDS on boron-doped diamond (BDD) thin-film electrodes [51]. The discovery of a non-radical pathway for PDS activation has updated people's understanding of the activation mechanism of PDS and promoted the further exploration of new catalytic materials. At present, great progress has been made in the research of several effective anode materials in PS activation process, such as BDD [25,28,42,43,53–57], Ti/IrO_2-Ta_2O_5 [43], SnO_2/Ni@NCNT [58], B-TNT anode [54], and carbon-based anode [59–62]. There are currently two main forms of non-radical pathways, which correspond to distinct PDS activation processes. Among them, electrocatalytic activation of PDS to generate $^1O_2$ is the main research object. Furthermore, in some special systems, activation of PDS can only occur by electron transfer. These findings are discussed in detail below. The radical pathway generates strongly reactive radicals ($^{\bullet}OH$, $SO_4^{\bullet-}$ and superoxide radicals ($O_2^{\bullet-}$)) through electrocatalytic activation of PDS. In addition to activating PDS to generate active species to remove pollutants, scholars have also found in situ generation of PDS on BDD anodes in sulphate electrolytes [Eqs. (8)–(10)] [42,43], it would be beneficial for cost reduction. In addition, PDS was also confirmed to generate $SO_4^{\bullet-}$ [Eq. (7)] during cathodic activation, broadening the application range of PDS.

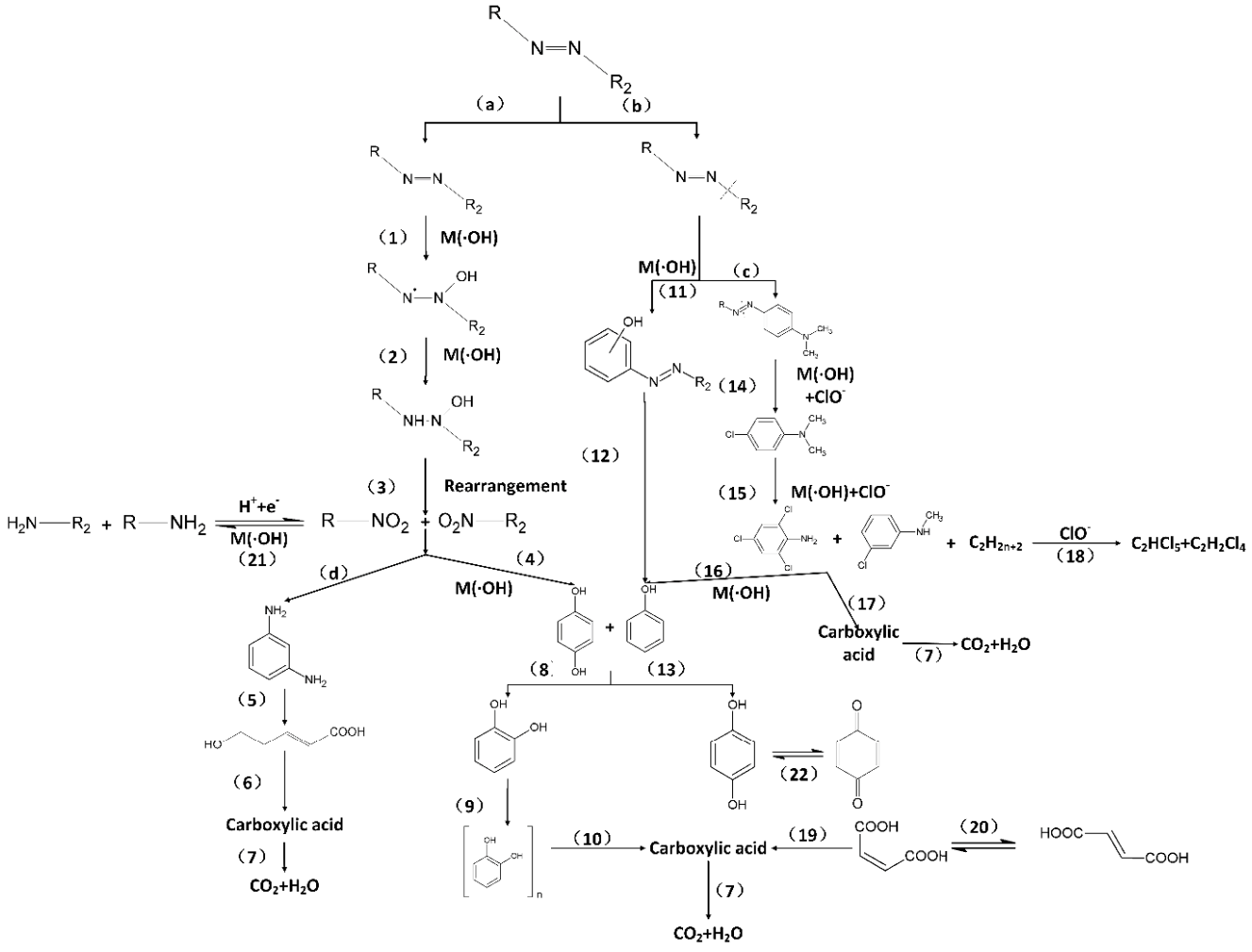

Fig. 3. General degradation process of azo compounds (R and R′ represent different aromatic groups, respectively) [81,82,84–87].

$$S_2O_8^{2-} + e^- \rightarrow SO_4^{2-} + SO_4^{-\bullet} \quad (7)$$

$$HSO_4^- - e^- \xrightarrow{BDD} \frac{1}{2}S_2O_8^{2-} + H^+ \quad (8)$$

$$SO_4^{2-} - e^- \xrightarrow{BDD} \frac{1}{2}S_2O_8^{2-} \quad (9)$$

$$SO_4^{2-} + SO_4^{\bullet-} \rightarrow S_2O_8^{2-} + e^- \quad (10)$$

The radical and non-radical oxidation mechanisms of the anodic surface activated PDS [Eqs. (11)–(17)] are as follows [63,64]:

$$HSO_4^- + M(^\bullet OH) \leftrightarrow M(SO_4^{-\bullet}) + H_2O \quad (11)$$

$$S_2O_8^{2-} \xrightarrow{abs} SO_4^{2-} - e^- \rightarrow M(SO_4^{-\bullet}) \quad (12)$$

$$2S_2O_8^{2-} + 6M(^\bullet OH) \xrightarrow{BDD} 4SO_4^{2-} + 2O_2^{-\bullet} + {}^1O_2 + 6H^+ \quad (13)$$

$$M(SO_4^{-\bullet}) + H_2O \rightarrow {}^\bullet OH + HSO_4^- \quad (14)$$

$$M(SO_4^{-\bullet}) + OH^- \rightarrow {}^\bullet OH + SO_4^{2-} \quad (15)$$

$$2M(SO_4^{-\bullet}) \rightarrow S_2O_8^{2-} \quad (16)$$

In order to determine the active species produced by PS and the reasons for its strong oxidative properties, many scholars have analyzed the activation mechanism of PS and the interaction between active species in different materials and degradation systems. Li et al. [65] found a synergistic effect between $^1O_2$ (non-radical pathway) and $SO_4^{\bullet-}$ (radical pathway). Ding et al. [66] found that the active sites of the three transition metals (Fe, Co, and Ti) on the catalyst surface can achieve a clear synergistic activation effect and induce the coexistence of $SO_4^{\bullet-}$ and OH. Li et al. [40] found that even though the transition metals in the $CuFe_2O_4$ catalyst entered the solution in an ionic state, these dissolved iron and copper ions would still be converted to $SO_4^{\bullet-}$ by activating PS. Furthermore, they found that $SO_4^{\bullet-}$ and H_2O could react to form OH under rebasication conditions, which was also confirmed by other studies [67,68]. Notably, some studies have found the opposite. Bu et al. [53] studied the degradation of ATZ in the BDD/PS system, and they found that the degradation effect decreased with increasing pH. They believe that this result is caused by the higher oxygen evolution overpotential in the acidic environment. Song et al. [69] found that the participation of PDS slightly inhibited the degradation of ATZ and methylene blue (NB) in the Ti/Pt anodic PDS system, which was inconsistent with the pattern of other persistent pollutants, and considered it to be PDS is a direct electro-oxidative competition on the electrode surface between ATZ and NB.

Carbon materials are good catalysts for activating PS. Some studies have found that sp2 hybrid carbon (C=O) is the main active site, while sp3 hybrid carbon (CH, $=CH_2$, C–OH) cannot activate PS [70]. Song et al. [54] determined that the active species is not the heterogeneous activation of PS by carbon materials, but originates from electrochemical reactions of PS that take place on the surface of carbon materials. During the electrochemical activation of PS, the anodic discharge can convert the adsorbed PDS or PMS molecules into a special transition-state structure PDS*/PMS* [Eq. (17)]. Unlike stable PDS or PMS molecules, PDS*/PMS* is in an activated state and is highly reactive.

$$PDS/PMS + BDD \rightarrow BDD(PDS^* / PMS^*) \quad (17)$$

A similar phenomenon was found on Pt anodes, Song et al. [69] demonstrated the existence of a special transition state $M(^*S_2O_8^{2-})$ on the Ti/Pt anode surface. Unlike the active sites of carbon materials, PDS adsorbed on the Pt anode is thought to form a transition state induced by the electric double layer discharge. PDS does not directly provide electrons, but changes the electronic structure through the flow of electrons during the discharge process of the electric double layer, transforming into a transition state. When a suitable electron donor is available, the activated PDS molecules are rapidly converted to SO_4^{2-}, which is consistent with the conclusions obtained for the BDD anode. Notably, PS can form a similar transition state in the carbon catalyst/PS/phenol system without electroactivation. In this system, electrons are spontaneously transferred from phenol (electron donor) to PDS (electron acceptor) through a specific carbon material (electron mediator) to activate PDS [71]. However, this phenomenon of direct electron transfer has not yet been discovered on BDD [54].

In subsequent studies, scholars confirmed that the active species in the carbon catalyst/PS/phenol system were mainly $^1O_2$ generated by the decomposition of PS [72]. The sites for the activation of PS by carbon catalysts mainly exist at edges/vacancies (pyridine nitrogen and pyrrolic nitrogen) [73], oxygen activation (C=O) [74], and doped heteroatoms (graphite nitrogen) [75]. Different dopant atoms also lead to different propensities for non-radical mechanisms. For example, in N-doped biochar (NBC), pyridine and pyrrolic nitrogen act as PS activation sites. But activation will not only produce $^1O_2$, but also produce a variety of active substances [76]. However, such studies are only significant for the treatment of phenol-containing wastewater, and such phenomena have not been found in other pollutants.

In addition to self-activation to generate active species, its adsorption at the active site also affects the activation of other species. Zhou et al. [77] discovered for the first time that PS facilitates the direct one-electron generation of atoms H* and $^1O_2$ for the degradation of tetracycline (TTC) via cathodic electroactivation of $MnFe_3O_4$@PZS core-shell catalysts. Manganese-oxygen bonds (Mn–O), pyridine nitrogen and sulfur-oxygen bonds (S=O) are the adsorption sites for H_2O and O_2. The presence of Mn and PS facilitates the direct one-electron transfer of adsorbed H_2O and O_2 to generate atomic H* and $^1O_2$ [Eqs. (18)–(20)].

This discovery expands the scope of non-radical processing mechanisms for organic pollutants.

$$O_2 + e^- \rightarrow {}^{\bullet}O_2^- / {}^{\bullet}HO_2^- \quad (18)$$

$${}^{\bullet}O_2^- / {}^{\bullet}HO_2^- \rightarrow {}^1O_2 \quad (19)$$

$$S_2O_8^{2-} + H_2O + e^- \rightarrow SO_{4\bullet}^- + {}^{\bullet}OH \rightarrow HSO_4^- + {}^1O_2 \quad (20)$$

3. Summary of the degradation process of azo dyes

Azo dyes are the most widely used synthetic organic dyes in the textile industry and are usually found in printing and dyeing wastewater. The chemical composition of azo dyes consists of alternating aromatic groups and azo bonds (–N=N–). Since –N=N– can absorb visible light of a certain frequency, it can be used as dye, acid–base indicator and metal indicator [78–83]. Most azo dyes will decompose under specific conditions of the human body to produce various aromatic amines [83], which have carcinogenic effects on the human body. Therefore, in addition to the strict control and use of azo dyes, the treatment and detoxification of dye wastewater is an essential link. Due to its low energy consumption and high degradation efficiency, electrochemical oxidation has become an important method for the removal of azo dyes.

The two ends of –N=N– in the azo dye molecule are connected with different aromatic groups, and there are various other functional groups on these aromatic rings, so it is difficult to mineralize from macromolecular azo compounds to inorganic substances. According to the group characteristics shared by the azo compound family, the process of OH oxidative degradation to azo compounds can be simply summarized into three stages: –N=N– destruction; evolution and ring opening of aromatic compounds; mineralization of small molecular carboxylic acids. Fig. 3 shows the main process of mineralization of azo compounds, clearly showing the general law of azo compounds being oxidized by OH. This section also mentions some specific decomposition processes.

Indirect electrooxidation generates a large number of oxidative active species (mainly OH) to attack the azo compound molecules, mainly attacking the conjugated structure of –N=N– and aromatic rings [81], so this indicates that the active species can have two attack sites dots (shown in paths (a) and (b)), one attacks the azo side of the macro-conjugated system and the other attacks the aromatic side (usually the benzene ring) [85].

3.1. Middle of the azo bond

Pathway (a) in Fig. 3, there are two cases: one is the ring-opening reaction of the naphthalene ring; the other is the evolution of the nitrogen on the benzene ring.

The ring-opening of naphthalene is dominated by OH attack [86]. The ring-opening reaction is mainly divided into three stages: (1) OH oxidation removes some nitrogen-containing sulfur-containing groups on the naphthalene ring, and an unsubstituted environment is obtained on a certain ring of the naphthalene ring; (2) The unsubstituted OH will The epoxidation of the base opens the ring to obtain a benzene ring substituted by a dicarboxylic acid (i.e., phthalic acid); (3) OH terephthalic acid is further oxidized to remove the substituent, and the oxidation ring is opened to obtain a small molecular carboxylic acid.

The nitrogen on the benzene ring can be interconverted between the amine group ($–NH_3$) and the nitro group ($–NO_2$) [Reaction (21)], $–NH_3$ is oxidized from OH to $–NO_2$, and conversely, by protons and solvated electrons (e^-), the latter is a complex alternating attack process headed by $–NH_3$ protonation [84,86]. Intermediates generated during the mutual evolution of $–NH_3$ and $–NO_2$ groups can also polymerize, polymerizing two benzene rings into a naphthalene ring. This evolution will not last forever, as OH can convert aniline- or nitrobenzene-based intermediates to phenols, diphenols [Eqs. (4), (12), (16)], and unsaturated hydroxycarboxylic acids [Reaction (5) in pathways (d)]. It should be noted that the evolutionary incarnation process leads to the production of macromolecular polymers, which form a polymer film on the electrode surface, which greatly reduces the degradation efficiency. Reaction (1) initiated by pathway (a) leads to the formation of an unstable transition state –N–N(OH)– which will further combine with OH to form –NH–N(OH)– [Fig. 3 Reaction (2)]. Therefore, N is dissociated from the macroscopic conjugated system. –NH–N(OH)– is not stable [82], it can rearrange to open N–N bonds to give final products – arylamines, nitroarenes and their copolymers. In the studies of Wang et al. [81], Zhang et al. [82], Thomas et al. [85] and Florenza et al. [86], the decolorization rates of the azo dyes all reached high values in a relatively short period of time, indicating that the attack rate of OH on the azo side is high and the speed is also fast.

Although the possibility of OH attacking the azo side is high, the most critical process affecting the degradation effect often occurs in other cases, which is caused by the formation of refractory intermediates, so comprehensive degradation process analysis is particularly important.

3.2. Both ends of the azo bond

Fig. 3 Path (b) is another location for an OH attack. Unlike route (a), this route OH attacks the benzene ring of the large conjugated system, so –N=N– must donate an electron to reach a new stable state, resulting in the cleavage of C–N [Reaction (12)]. But this pathway requires a strong electron withdrawing group attached to the aromatic ring at the other end of –N=N– to reduce the electron cloud density on –N=N– for activation [74]. This pathway produces another intermediate, phenol, in the degradation of azo compounds.

If the supporting electrolyte under degradation conditions is chloride ions (i.e., the degradation process is an indirect electrooxidation involving active chlorine), route (b) presents another special case in which the active chlorine species may also attack the C–N bond [Reactions (14)–(16)], which requires attention because the resulting organochlorine derivatives are extremely difficult to degrade further and these compounds are still dangerous [Reaction (18)] [3,81]. For example, when Ding et al. [37] studied the

degradation process of bisphenol A involving chlorine-active substances, he found that the organochlorine derivatives ($C_6H_3Cl_3O$) produced during the degradation process were more toxic than untreated bisphenol A.

With the disintegration of –N=N–, azo compounds gradually evolve into aromatic intermediates, which have been mentioned in the previous section. Most aromatic intermediates are aromatic amines, nitroarenes and their polymers, and phenols. They cannot exist for a long time in the presence of strong oxidative active substances such as OH, and further oxidize and open the ring to generate small molecular carboxylic acids. For pathways (a) and (b), OH-dominant oxidation occurs at a faster rate, oxidizing aniline and nitrobenzene intermediates to diphenols. The diphenol is further oxidized by OH to open the ring to obtain a small molecular carboxylic acid. Among the resulting diphenols, catechol and hydroquinone undergo Reactions (9), (10) and (22), (19), (20), respectively, to form small carboxylic acids such as malic acid, malonic acid, acetic acid, oxalic acid and formic acid [87].

3.3. Quantum chemical calculations for prediction of oxidation mechanisms

The growing number of emerging pollutants in the environment requires an efficient approach to facilitate reactivity prediction and gain insight into reaction mechanisms. Quantum chemical calculation is a tool to meet this demand, and it has a good performance in the theoretical study of chemical reactions at the molecular level. Modern computational chemistry is based on quantum mechanics and computer technology to explain and predict the properties of molecules or to speculate on the starting conditions of reactions [88]. Commonly used methods include wave function theory (Hartree-Fock and post-Hartree-Fock methods), density functional theory (DFT), semi-empirical and other computational methods [88]. Quantum chemical calculations, especially using DFT methods, can be applied to larger molecular systems with thousands of atoms [89]. Compared with semi-empirical methods, DFT calculations can describe geometric, electronic structure and spectral properties well. While both wave function theory and DFT are first-principles methods, unlike wave function methods, DFT does not solve Hartree-Fock-Rothaan equations followed by Hartree-Fock processing (such as configuration interactions and Møller-Plesset perturbation theory), instead considering the ground state energy as the electron density, so that all other electronic properties in the system can be broadly determined [90]. This method makes the DFT calculation faster than the wave function theory method. In most cases, the DFT results are in good agreement with the experiments. Therefore, DFT has become the most popular quantum chemical calculation method in current computer architectures. At present, the most widely used DFT first-principles calculation methods mainly include quantitative structure-activity relationship (QSAR), quantitative structure-activity relationship (QSPR), linear free energy relationship (LFER) and group contribution method (GCM) [89–92].

A Asghar et al. [5] used quantum chemical analysis to predict the degradation potential of the recalcitrant dye Acid Blue 113 for H_2O_2, O_3, OH and $SO_4^{\bullet-}$. Natural bond orbital analysis shows that acid blue 113 is highly structurally stable due to its strong intermolecular and intramolecular interactions. They then compared the reactivity of dyes with oxidants based on the highest occupied molecular orbital (HOMO) and lowest unoccupied molecular orbital (LUMO) energy values. The results show that acid blue 113 is nucleophilic and easily degraded by O_3 and OH due to the lower HOMO-LUMO energy gap of O_3 and OH. In contrast, the HOMO-LUMO gaps of $SO_4^{\bullet-}$ and H_2O_2 are 7.92 and 8.10 eV, respectively, indicating that they are not easily degraded by acid blue 113. This study shows that quantum chemical analysis can effectively aid in the selection of suitable active substances to treat organic dye wastewater.

Since DFT is computationally intensive, most of the computations are usually performed in ultra-vacuum systems. However, during the electrochemical process, an electric double layer structure exists on the electrode surface. This structure is different from an ultra-vacuum system. The composition (solvent and solute) and the ability to form a local electric field at the electrode surface interfere with the calculation of the electrochemical potential (μ_e) and total electron number (N_e), and affect the total free energy (Φ) of the electrode surface [93–96]. To ensure that the calculated results are closer to the actual electrochemical system, pure DFT will not be applicable and hybrid DFT calculations will be required, such as hybrid quantum mechanics/molecular mechanics (QM/MM) [97,98] methods that use force fields to treat the solvent/electrolyte atoms, and continuum methods [99] that treat the solvent/electrolyte using only density and charge distribution. Shi et al. [100] summarized the effect of water on the adsorption energy of OER intermediates in DFT calculations and concluded that solvation-corrected DFT calculations were more accurate than pure DFT calculations. R G González-Huerta et al. [92] used electrochemical polarization and DFT to analyze the kinetic pathways of OER on RuO_2, IrO_2 and RuIrCoOx surfaces and the role of catalysts in the first fundamental reaction of OER. They found that the RuIrCoOx surface displayed the lowest Tafel slope values and that the rate-determining step at low overpotentials was the second H–O scission (Eq. 22). The study identified a change in the electronic structure of the slower reaction in the second-step compared to the first step (Eq. 21).

$$M + H_2O \rightarrow M\left(^{\bullet}OH\right) + H^+ + e^- \tag{21}$$

$$M\left(^{\bullet}OH\right) \rightarrow MO + H^+ + e^- \tag{22}$$

4. Summary and outlook

Since O_v generates OH through the adsorption and dehydrogenation of water molecules on the surface of the anode material, the amount of O_v and its binding energy with intermediates can affect the adsorption, dissociation and desorption of H_2O and its intermediates. Therefore, finding anode materials with more Ov and lowering their binding energy with OH is one of the key factor to obtain good degradation efficiency.

With the deepening of the research on the PS oxidation mechanism, the research on carbon materials has gradually become the focus. In a BDD/PS system, PS can be generated in situ on the BDD. Electron transfer and $^1O_2$ promote degradation in a specific non-electrocatalytic system (carbon material + PS + phenol). In addition, there is a synergistic effect of degrading pollutants between the free radical oxidation process and the non-radical oxidation process, but the mechanism of this effect is not clear. DFT, especially solvent-calibrated DFT, can predict the main degradation process of organics and the activation mechanism of the catalyst surface, so the mechanism of the synergistic reaction can be further predicted by these methods.

In addition to the effect of active substances on degradation, the decomposition process of organic dyes also has an important influence on its degradation effect. Although the potential for the active species to attack the azo side is high, the key processes affecting the degradation effect often occur elsewhere. These refractory intermediates will lead to a decrease in mineralization efficiency, and some intermediates are even more toxic than undegraded precursors, so it is necessary to strengthen the research on these intermediates.

Acknowledgments

Funding: This work was supported by Natural Science Foundation of Shanghai [Grant Nos. 20ZR1421500]; Science and Technology Commission of Shanghai Municipality [19DZ2271100].

Declaration of competing interest

The authors declare that they have no known competing financial interests or personal relationships that could have appeared to influence the work reported in this paper.

References

[1] I. Novak, Photoelectron spectroscopy of organic pollutants: chlorophenols, J. Electron. Spectrosc. Relat. Phenom., 239 (2020) 146919, doi: 10.1016/j.elspec.2019.146919.
[2] Z. Hao, H.T. Xu, Z.Y. Feng, C.C. Zhang, X. Zhou, Z.F. Wang, J.H. Zheng, X.Q. Zou, Spatial distribution, deposition flux, and environmental impact of typical persistent organic pollutants in surficial sediments in the Eastern China Marginal Seas (ECMSs), J. Hazard. Mater., 407 (2021) 124343, doi: 10.1016/j.jhazmat.2020.124343.
[3] E. Brillas, C.A. Martinez-Huitle, Decontamination of wastewaters containing synthetic organic dyes by electrochemical methods. An updated review, Appl. Catal., B, 166 (2015) 603–643.
[4] V.L. Prasanna, H. Mamane, V.K. Vadivel, D. Avisar, Ethanol-activated granular aerogel as efficient adsorbent for persistent organic pollutants from real leachate and hospital wastewater, J. Hazard. Mater., 384 (2020) 121396, doi: 10.1016/j.jhazmat.2019.121396.
[5] A. Asghar, M.M. Bello, A.A. Raman, W.M.A.W. Daud, A. Ramalingam, S.B. Zain, Predicting the degradation potential of Acid blue 113 by different oxidants using quantum chemical analysis, Heliyon, 5 (2019) e02396, doi: 10.1016/j.heliyon.2019.e02396.
[6] R. Kishor, D. Purchase, G.D. Saratale, R.G. Saratale, L.F.R. Ferreira, M. Bilal, R. Chandra, R.N. Bharagava, Ecotoxicological and health concerns of persistent coloring pollutants of textile industry wastewater and treatment approaches for environmental safety, J. Environ. Chem. Eng., 9 (2021) 105012, doi: 10.1016/j.jece.2020.105012.
[7] P. Mandal, B.K. Dubey, A.K. Gupta, Review on landfill leachate treatment by electrochemical oxidation: drawbacks, challenges and future scope, Waste Manage., 69 (2017) 250–273.
[8] V. Vaezzadeh, M.W. Thomes, T. Kunisue, N.M. Tue, G. Zhang, M.P. Zakaria, Y.A. Affendi, F.C. Yap, L.L. Chew, H.W. Teoh, C.W. Lee, C.W. Bong, Examination of barnacles' potential to be used as bioindicators of persistent organic pollutants in coastal ecosystem: a Malaysia case study, Chemosphere, 263 (2021) 128272, doi: 10.1016/j.chemosphere.2020.128272.
[9] P.E. Payandeh, N. Mehrdadi, P. Dadgar, Study of biological methods in landfill leachate treatment, Open J. Ecol., 7 (2017) 568–580.
[10] S. Renou, J.G. Givaudan, S. Poulain, F. Dirassouyan, P. Moulin, Landfill leachate treatment: review and opportunity, J. Hazard. Mater., 150 (2008) 468–493.
[11] F. Di Capua, F. Adani, F. Pirozzi, G. Esposito, A. Giordano, Air side-stream ammonia stripping in a thin film evaporator coupled to high-solid anaerobic digestion of sewage sludge: process performance and interactions, J. Environ. Manage., 295 (2021) 113075, doi: 10.1016/j.jenvman.2021.113075.
[12] L. Miao, G. Yang, T. Tao, Y.Z. Peng, Recent advances in nitrogen removal from landfill leachate using biological treatments – a review, J. Environ. Manage., 235 (2019) 178–185.
[13] Y. Deng, N. Chen, W. Hu, H.S. Wang, P.J. Kuang, F.X. Chen, C.P. Feng, Treatment of old landfill leachate by persulfate enhanced electro-coagulation system: improving organic matters removal and precipitates settling performance, Chem. Eng. J., 424 (2021) 130262, doi: 10.1016/j.cej.2021.130262.
[14] M.A.M. Reshadi, A. Bazargan, G. Mckay, A review of the application of adsorbents for landfill leachate treatment: focus on magnetic adsorption, Sci. Total Environ., 731 (2020) 138863, doi: 10.1016/j.scitotenv.2020.138863.
[15] Q.T. An, Z. Zhang, H.H. Su, X. Li, Review on landfill leachate treatment methods, IOP Conf. Ser.: Earth Environ. Sci., 565 (2020) 012038, doi: 10.1088/1755-1315/565/1/012038.
[16] B.P. Chang, A. Gupta, T.H. Mekonnen, Flame synthesis of carbon nanoparticles from corn oil as a highly effective cationic dye adsorbent, Chemosphere, 282 (2021) 131062, doi: 10.1016/j.chemosphere.2021.131062.
[17] H.-Z. Li, Y.-N. Zhang, J.-Z. Guo, J.-Q. Lv, W.-W. Huang, B. Li, Preparation of hydrochar with high adsorption performance for methylene blue by co-hydrothermal carbonization of polyvinyl chloride and bamboo, Bioresour. Technol., 337 (2021) 125442, doi: 10.1016/j.biortech.2021.125442.
[18] A. Fallahi, F. Rezvani, H. Asgharnejad, E.K. Nazloo, N. Hajinajaf, B. Higgins, Interactions of microalgae-bacteria consortia for nutrient removal from wastewater: a review, Chemosphere, 272 (2021) 129878, doi: 10.1016/j.chemosphere.2021.129878.
[19] P.R. Shukla, S. Wang, H. Sun, H.M. Ang, M. Tade, Activated carbon supported cobalt catalysts for advanced oxidation of organic contaminants in aqueous solution, Appl. Catal., B, 100 (2010) 529–534.
[20] F. Wei, D. Liao, Y. Lin, C. Hu, J.Q. Ju, Y.S. Chen, D.L. Feng, Electrochemical degradation of reverse osmosis concentrate (ROC) using the electrodeposited Ti/TiO_2-NTs/PbO_2 electrode, Sep. Purif. Technol., 258 (2021) 118056, doi: 10.1016/j.seppur.2020.118056.
[21] X. Liu, L. Min, X. Yu, Z. Zhou, L. Sha, S.T. Zhang, Changes of photoelectrocatalytic, electrocatalytic and pollutant degradation properties during the growth of β-PbO_2 into black titanium oxide nanoarrays, Chem. Eng. J., 417 (2021) 127996, doi: 10.1016/j.cej.2020.127996.
[22] S. Boukhchina, H. Akrout, D. Berling, L. Bousselmi, Highly efficient modified lead oxide electrode using a spin coating/electrode position mode on titanium for electrochemical treatment of pharmaceutical pollutant, Chemosphere, 221 (2019) 356–365.
[23] D. Guo, Y.B. Guo, Y.X. Huang, Y.Y. Chen, X.C. Dong, H. Chen, S.P. Li, Preparation and electrochemical treatment application of Ti/Sb–SnO_2-Eu&rGO electrode in the degradation of

clothianidin wastewater, Chemosphere, 265 (2021) 129126, doi: 10.1016/j.chemosphere.2020.129126.
[24] S. Man, H. Bao, H. Yang, K. Xu, A.Q. Li, Y.T. Xie, Y. Jian, W.J. Yang, Z.H. Mo, X.M. Li, Preparation and characterization of Nano-SiC doped PbO_2 electrode for degradation of toluene diamine, J. Alloys Compd., 859 (2021) 157884, doi: 10.1016/j.jallcom.2020.157884.
[25] M. Pierpaoli, P. Jakobczyk, M. Sawczak, A. Luczkiewicz, S. Fudala-Ksiazek, R. Bogdanowicz, Carbon nanoarchitectures as high-performance electrodes for the electrochemical oxidation of landfill leachate, J. Hazard. Mater., 401 (2021) 123407, doi: 10.1016/j.jhazmat.2020.123407.
[26] S. Chen, P. He, X. Wang, F. Xiao, P.C. Zhou, Q.H. He, L.P. Jia, F.Q. Dong, H. Zhang, B. Jia, H.T. Liu, B. Tang, Co/Sm-modified Ti/PbO_2 anode for atrazine degradation: effective electrocatalytic performance and degradation mechanism, Chemosphere, 268 (2021) 128799, doi: 10.1016/j.chemosphere.2020.128799.
[27] M. Chen, X. Zhao, C. Wang, S. Pan, C. Zhang, Y.C. Wang, Electrochemical oxidation of reverse osmosis concentrates using macroporous Ti-ENTA/SnO_2-Sb flow-through anode: degradation performance, energy efficiency and toxicity assessment, J. Hazard. Mater., 401 (2021) 123295, doi: 10.1016/j.jhazmat.2020.123295.
[28] J. Cai, M. Zhou, X. Du, X. Xu, Enhanced mechanism of 2,4-dichlorophenoxyacetic acid degradation by electrochemical activation of persulfate on blue-TiO_2 nanotubes anode, Sep. Purif. Technol., 254 (2021) 117560, doi: 10.1016/j.seppur.2020.117560.
[29] W. Zhou, X. Meng, J. Gao, A.N. Alshawabkeh, Hydrogen peroxide generation from O_2 electroreduction for environmental remediation: a state-of-the-art review, Chemosphere, 225 (2019) 588–607.
[30] J. Zhang, W. Zhou, L. Yang, Y.C. Chen, Y.Y. Hu, Co-N-doped MoO_2 modified carbon felt cathode for removal of EDTA-Ni in electro-Fenton process, Environ. Sci. Pollut. Res., 25 (2018) 22754–22765.
[31] K. Zhu, J. Ouyang, J.M. Liu, Y.X. Zhu, Q. Zeng, Y.J. Cui, Preparation and photocatalytic hydrogen evolution from water of oxygen doped carbon nitride nanosheets, Chin. J. Inorg. Chem., 35 (2019) 1005–1012.
[32] M.A. Radi, N. Nasirizadeh, M. Rohani-Moghadam, M. Dehghani, The comparison of sonochemistry, electrochemistry and sonoelectrochemistry techniques on decolorization of C.I. Reactive Blue 49, Ultrason. Sonochem., 27 (2015) 609–615.
[33] M. Sharma, A. Halder, R. Vaish, Effect of Ce on piezo/photocatalytic effects of $Ba_{0.9}Ca_{0.1}Ce_xTi_{1-x}O_3$ ceramics for dye/pharmaceutical waste water treatment, Mater. Res. Bull., 122 (2020) 110647, doi: 10.1016/j.materresbull.2019.110647.
[34] R. Li, X.K. Lu, B.B. Yan, N. Li, G.Y. Chen, Z.J. Cheng, L.A. Hou, S.B. Wang, X.G. Duan, Sludge-derived biochar toward sustainable peroxymonosulfate activation: regulation of active sites and synergistic production of reaction oxygen species, Chem. Eng. J., 440 (2022) 135897, doi: 10.1016/j.cej.2022.135897.
[35] Y. Yang, L.C. Kao, Y.Y. Liu, K. Sun, H.T. Yu, J.H. Guo, S.Y.H. Liou, M.R. Hoffmann, Cobalt-doped black TiO_2 nanotube array as a stable anode for oxygen evolution and electrochemical wastewater treatment, ACS Catal., 8 (2018) 4278–4287.
[36] L.Y. Wu, Q. Zhang, J.M. Hong, Z.Y. Dong, J. Wang, Degradation of bisphenol A by persulfate activation via oxygen vacancy-rich $CoFe_2O_{4-x}$, Chemosphere, 221 (2019) 412–422.
[37] J. Ding, L.J. Bu, Q.L. Zhao, F.T. Kabutey, L.L. Wei, D.D. Dionysiou, Electrochemical activation of persulfate on BDD and DSA anodes: electrolyte influence, kinetics and mechanisms in the degradation of bisphenol A, J. Hazard. Mater., 388 (2020) 121789, doi: 10.1016/j.jhazmat.2019.121789.
[38] J. Cai, M. Zhou, Y. Pan, X.D. Du, X.Y. Lu, Extremely efficient electrochemical degradation of organic pollutants with co-generation of hydroxyl and sulfate radicals on blue-TiO_2 nanotubes anode, Appl. Catal., B, 257 (2019) 117902, doi: 10.1016/j.apcatb.2019.117902.
[39] J. Zuo, J. Zhu, M. Zhang, Q.M. Hong, J. Han, J.F. Liu, Synergistic photoelectrochemical performance of La-doped RuO_2-TiO_2/Ti electrodes, Appl. Surf. Sci., 502 (2020) 144288, doi: 10.1016/j.apsusc.2019.144288.
[40] J. Li, J.F. Yan, G. Yao, Y.H. Zhang, X. Li, B. Lai, Improving the degradation of atrazine in the three-dimensional (3D) electrochemical process using $CuFe_2O_4$ as both particle electrode and catalyst for persulfate activation, Chem. Eng. J., 361 (2019) 1317–1332.
[41] J.L. Wang, S.Z. Wang, Reactive species in advanced oxidation processes: formation, identification and reaction mechanism, Chem. Eng. J., 401 (2020) 126158, doi: 10.1016/j.cej.2020.126158.
[42] L.J. Bu, S.Q. Zhou, Z. Shi, L. Deng, N.Y. Gao, Removal of 2-MIB and geosmin by electrogenerated persulfate: performance, mechanism and pathways, Chemosphere, 168 (2017) 1309–1316.
[43] S.Q. Zhou, L.J. Bu, Y.H. Yu, X. Zou, Y.S. Zhang, A comparative study of microcystin-LR degradation by electrogenerated oxidants at BDD and MMO anodes, Chemosphere, 165 (2016) 381–387.
[44] A. Kowal, M. Li, M. Shao, K. Sasaki, M.B. Vukmirovic, J. Zhang, N.S. Marinkovic, P. Liu, A.I. Frenkel, R.R. Adzic, Ternary Pt/Rh/SnO_2 electrocatalysts for oxidizing ethanol to CO_2, Nat. Mater., 8 (2009) 325–330.
[45] L. Gan, Y. Wu, H. Song, C. Lu, S.P. Zhang, A.M. Li, Self-doped TiO_2 nanotube arrays for electrochemical mineralization of phenols, Chemosphere, 226 (2019) 329–339.
[46] X. Li, Z.K. Kou, J. Wang, Manipulating interfaces of electrocatalysts down to atomic scales: fundamentals, strategies, and electrocatalytic applications, Small Methods, 5 (2020) 2001010, doi: 10.1002/smtd.202001010.
[47] F. Zahmatkeshani, M. Tohidi, Synthesis of SnO_2, Zn-doped SnO_2 and Zn_2SnO_4 nanostructure-based hierarchical architectures by using deep eutectic precursors and their photocatalytic application, Cryst. Eng. Commun., 21 (2019) 6758–6771.
[48] R.Z. Xie, X.Y. Meng, P.Z. Sun, J.F. Niu, W.J. Jiang, L. Bottomley, D. Li, Y.S. Chen, J. Crittenden, Electrochemical oxidation of ofloxacin using a TiO_2-based SnO_2-Sb/polytetrafluoroethylene resin-PbO_2 electrode: reaction kinetics and mass transfer impact, Appl. Catal., B, 203 (2017) 515–525.
[49] M.Z. Wu, L.J. Lu, Y.B. Yang, Y. Chang, R.X. Chen, Y. Li, J. Du, C.Y. Tao, Z.H. Liu, Y.J. Liu, L. Gou, S.H. Pan, D. Ran, J. Li, A triethanolamine-assisted fabrication of stable Sb doped-SnO_2/Ti electrode for electrocatalytic oxidation of rhodamine B, Colloids Surf., A, 634 (2021) 127976, doi: 10.1016/j.colsurfa.2021.127976.
[50] A. Chen, S. Xia, Z. Ji, H.W. Lu, Insights into the origin of super-high oxygen evolution potential of Cu doped SnO_2 anodes: a theoretical study, Appl. Surf. Sci., 471 (2019) 149–153.
[51] C. Costentin, D.G. Nocera, C.N. Brodsky, Multielectron, multisubstrate molecular catalysis of electrochemical reactions: formal kinetic analysis in the total catalysis regime, Proc. Natl. Acad. Sci. U.S.A., 114 (2017) 11303–11308.
[52] X.B. Qian, K.F. Peng, L. Xu, S.Y. Tang, W.L. Wang, M. Zhang, J.F. Niu, Electrochemical decomposition of PPCPs on hydrophobic Ti/SnO_2-Sb/La-PbO_2 anodes: relationship between surface hydrophobicity and decomposition performance, Chem. Eng. J., 429 (2022) 132309, doi: 10.1016/j.cej.2021.132309.
[53] L.J. Bu, S.M. Zhu, S.Q. Zhou, Degradation of atrazine by electrochemically activated persulfate using BDD anode: role of radicals and influencing factors, Chemosphere, 195 (2018) 236–244.
[54] H.R. Song, L.X. Yan, J. Jiang, J. Ma, Z.X. Zhang, J.M. Zhang, P.X. Liu, T. Yang, Electrochemical activation of persulfates at BDD anode: radical or non-radical oxidation?, Water Res., 128 (2018) 393–401.
[55] N. Pueyo, M.P. Ormad, N. Miguel, P. Kokkinos, A. Ioannidi, D. Mantzavinos, Z. Frontistis, Electrochemical oxidation of butyl paraben on boron doped diamond in environmental matrices and comparison with sulfate radical-AOP, J. Environ. Manage., 269 (2020) 110783, doi: 10.1016/j.jenvman.2020.110783.
[56] J.J. Cai, M.H. Zhou, Y. Liu, A. Savall, K.G. Serrano, Indirect electrochemical oxidation of 2,4-dichlorophenoxyacetic acid using electrochemically-generated persulfate, Chemosphere, 204 (2018) 163–169.
[57] Y.U. Shin, H.Y. Yoo, Y.Y. Ahn, M.S. Kim, K. Lee, S. Yu, C. Lee, K. Cho, H.I. Kim, J. Lee, Electrochemical oxidation of organics in sulfate solutions on boron-doped diamond electrode:

multiple pathways for sulfate radical generation, Appl. Catal., B, 254 (2019) 156–165.
[58] P.Z. Duan, D.D. Chen, X. Hu, Tin dioxide decorated on Ni-encapsulated nitrogen-doped carbon nanotubes for anodic electrolysis and persulfate activation to degrade cephalexin: mineralization and degradation pathway, Chemosphere, 269 (2021) 128740, doi: 10.1016/j.chemosphere.2020.128740.
[59] S. Dimitriadou, Z. Frontistis, A. Petala, G. Bampos, D. Mantzavinos, Carbocatalytic activation of persulfate for the removal of drug diclofenac from aqueous matrices, Catal. Today, 355 (2020) 937–944.
[60] Y.-J. Shih, C.-P. Huang, Y.-H. Chan, Y.-H. Huang, Electrochemical degradation of oxalic acid over highly reactive nano-textured γ- and α-MnO_2/carbon electrode fabricated by $KMnO_4$ reduction on loofah sponge-derived active carbon, J. Hazard. Mater., 379 (2019) 120759, doi: 10.1016/j.jhazmat.2019.120759.
[61] M. Ferreira, I. Kuzniarska-Biernacka, A.M. Fonseca, I.C. Neves, O.S.G.P. Soares, M.F.R. Pereira, J.L. Figueiredo, P. Parpot, Electrochemical oxidation of amoxicillin on carbon nanotubes and carbon nanotube supported metal modified electrodes, Catal. Today, 357 (2020) 322–331.
[62] X. Duan, W. Wang, Q. Wang, X.Y. Sui, N. Li, L.M. Chang, Electrocatalytic degradation of perfluoroocatane sulfonate (PFOS) on a 3D graphene-lead dioxide (3DG-PbO_2) composite anode: electrode characterization, degradation mechanism and toxicity, Chemosphere, 260 (2020) 127587, doi: 10.1016/j.chemosphere.2020.127587.
[63] Y.Y. Ahn, H. Bae, H.I. Kim, S.H. Kim, J.H. Kim, S.G. Lee, J. Lee, Surface-loaded metal nanoparticles for peroxymonosulfate activation: efficiency and mechanism reconnaissance, Appl. Catal., B, 241 (2019) 561–569.
[64] A. Farhat, J. Keller, S. Tait, J. Radjenovic, Removal of persistent organic contaminants by electrochemically activated sulfate, Environ. Sci. Technol., 49 (2015) 14326–14333.
[65] Z. Li, Y.Q. Sun, Y. Yang, Y.T. Han, T.S. Wang, J.W. Chen, D.C.W. Tsang, Comparing biochar- and bentonite-supported Fe-based catalysts for selective degradation of antibiotics: mechanisms and pathway, Environ. Res., 183 (2020) 109156, doi: 10.1016/j.envres.2020.109156.
[66] M. Ding, W. Chen, H. Xu, Z. Shen, T. Lin, K. Hu, Q. Kong, G. Yang, Z.L. Xie, Heterogeneous $Fe_2CoTi_3O_{10}$-MXene composite catalysts: synergistic effect of the ternary transition metals in the degradation of 2,4-dichlorophenoxyacetic acid based on peroxymonosulfate activation, Chem. Eng. J., 378 (2019) 122177, doi: 10.1016/j.cej.2019.122177.
[67] L. Chen, C. Lei, Z. Li, B. Yang, X.W. Zhang, L.C. Lei, Electrochemical activation of sulfate by BDD anode in basic medium for efficient removal of organic pollutants, Chemosphere, 210 (2018) 516–523.
[68] X. Wu, X. Song, H. Chen, J.G. Yu, Treatment of phenolic compound wastewater using $CuFe_2O_4/Al_2O_3$ particle electrodes in a three-dimensional electrochemical oxidation system, Environ. Technol., 42 (2020) 4393–4404.
[69] H. Song, L. Yan, J. Ma, J. Jiang, G.Q. Cai, W.J. Zhang, Z.X. Zhang, J.M. Zhang, T. Yang, Nonradical oxidation from electrochemical activation of peroxydisulfate at Ti/Pt anode: efficiency, mechanism and influencing factors, Water Res, 116 (2017) 182–193.
[70] S. Garcia-Segura, E.V. Dos Santos, C.A. Martinez-Huitle, Role of sp^3/sp^2 ratio on the electrocatalytic properties of boron-doped diamond electrodes: a mini review, Electrochem. Commun., 59 (2015) 52–55.
[71] H. Lee, H.J. Lee, J. Jeong, J. Lee, N.B. Park, C. Lee, Activation of persulfates by carbon nanotubes: oxidation of organic compounds by nonradical mechanism, Chem. Eng. J., 266 (2015) 28–33.
[72] Y. Wang, M. Liu, X. Zhao, D. Cao, T. Guo, B. Yang, Insights into heterogeneous catalysis of peroxymonosulfate activation by boron-doped ordered mesoporous carbon, Carbon, 135 (2018) 238–247.
[73] X. Chen, W.D. Oh, T.T. Lim, Graphene- and CNTs-based carbocatalysts in persulfates activation: material design and catalytic mechanisms, Chem. Eng. J., 354 (2018) 941–976.
[74] C. Sun, T. Chen, Q. Huang, M.X. Zhan, X.D. Li, J.H. Yan, Activation of persulfate by CO_2-activated biochar for improved phenolic pollutant degradation: performance and mechanism, Chem. Eng. J., 380 (2020) 122519, doi: 10.1016/j.cej.2019.122519.
[75] S. Liu, Z. Zhang, F. Huang, Y.Z. Liu, L. Feng, J. Jiang, L.Q. Zhang, F. Qi, C. Liu, Carbonized polyaniline activated peroxymonosulfate (PMS) for phenol degradation: role of PMS adsorption and singlet oxygen generation, Appl. Catal., B, 286 (2021) 119921, doi: 10.1016/j.apcatb.2021.119921.
[76] H. Wang, W. Guo, B. Liu, Q.L. Wu, H.C. Luo, Q. Zhao, Q.S. Si, F. Sseguya, N.Q. Ren, Edge-nitrogenated biochar for efficient peroxydisulfate activation: an electron transfer mechanism, Water Res., 160 (2019) 405–414.
[77] H. Zhou, D. Lu, S. Fang, L. Chang, Y.C. Chen, Y.Y. Hu, Q.J. Luo, Prompting direct single electron transfer to produce non-radical $^1O_2$/H* by electro-activating peroxydisulfate process with core-shell cathode, J. Environ. Manage., 287 (2021) 112294, doi: 10.1016/j.jenvman.2021.112294.
[78] Y.F. Song, J.M. Liu, F. Ge, X. Huang, Y. Zhang, H.H. Ge, X.J. Meng, Y.Z. Zhao, Influence of Nd-doping on the degradation performance of Ti/Sb-SnO_2 electrode, J. Environ. Chem. Eng., 9 (2021) 105409, doi: 10.1016/j.jece.2021.105409.
[79] G. Sun, C. Wang, W. Gu, Q.J. Song, A facile electroless preparation of Cu, Sn and Sb oxides coated Ti electrode for electrocatalytic degradation of organic pollutants, Sci. Total Environ., 772 (2021) 144908, doi: 10.1016/j.scitotenv.2020.144908.
[80] S. Yu, C. Hao, Z. Li, R.R. Zhang, Y. Dang, J.J. Zhu, Promoting the electrocatalytic performance of PbO_2 nanocrystals via incorporation of Y_2O_3 nanoparticles: degradation application and electrocatalytic mechanism, Electrochim. Acta, 369 (2021) 137671, doi: 10.1016/j.electacta.2020.137671.
[81] G.R. Wang, Y. Liu, J.W. Ye, Z.F. Lin, X.J. Yang, Electrochemical oxidation of methyl orange by a Magnéli phase Ti_4O_7 anode, Chemosphere, 241 (2020) 125084, doi: 10.1016/j.chemosphere.2019.125084.
[82] X. Zhang, D. Shao, W. Lyu, G.Q. Tan, H.J. Ren, Utilizing discarded SiC heating rod to fabricate SiC/Sb-SnO_2 anode for electrochemical oxidation of wastewater, Chem. Eng. J., 361 (2019) 862–873.
[83] Y. Xia, G. Wang, L. Guo, Q.Z. Dai, X.J. Ma, Electrochemical oxidation of Acid Orange 7 azo dye using a PbO_2 electrode: parameter optimization, reaction mechanism and toxicity evaluation, Chemosphere, 241 (2020) 125010, doi: 10.1016/j.chemosphere.2019.125010.
[84] N. Jiang, Y.C. Wang, Q.L. Zhao, Z.F. Ye, Application of Ti/IrO_2 electrode in the electrochemical oxidation of the TNT red water, Environ. Pollut., 259 (2020) 113801, doi: 10.1016/j.envpol.2019.113801.
[85] S. Thomas, R. Sreekanth, V.A. Sijumon, U.K. Aravind, C.T. Aravindakumar, Oxidative degradation of Acid Red 1 in aqueous medium, Chem. Eng. J., 244 (2014) 473–482.
[86] X. Florenza, A.M.S. Solano, F. Centellas, C.A. Martinez-Huitle, E. Brillas, S. Garcia-Segura, Degradation of the azo dye Acid Red 1 by anodic oxidation and indirect electrochemical processes based on Fenton's reaction chemistry. Relationship between decolorization, mineralization and products, Electrochim. Acta, 142 (2014) 276–288.
[87] W.Y. Wu, Z.H. Huang, T.T. Lim, Recent development of mixed metal oxide anodes for electrochemical oxidation of organic pollutants in water, Appl. Catal., A, 480 (2014) 58–78.
[88] G.A. McCarver, T. Rajeshkumar, K.D. Vogiatzis, Computational catalysis for metal-organic frameworks: an overview, Coord. Chem. Rev., 436 (2021) 213777, doi: 10.1016/j.ccr.2021.213777.
[89] C. Shao, F. Zhang, X. Li, J.H. Zhang, Y.S. Jiang, H.Y. Cheng, K.G. Zhu, Influence of Cr doping on the oxygen evolution potential of SnO_2/Ti and Sb-SnO_2/Ti electrodes, J. Electroanal. Chem., 832 (2019) 436–443.
[90] W. Fu, G.-J. Xia, Y. Zhang, J.H. Hu, Y.-G. Wang, J. Li, X.Y. Li, B. Li, Using general computational chemistry strategy to unravel the reactivity of emerging pollutants: an example of sulfonamide chlorination, Water Res., 202 (2021) 117391, doi: doi: 10.1016/j.watres.2021.117391.

[91] M. Behrens, F. Studt, I. Kasatkin, S. Kuehl, M. Haevecker, F. Abild-Pedersen, S. Zander, F. Girgsdies, P. Kurr, B.L. Kniep, The active site of methanol synthesis over $Cu/ZnO/Al_2O_3$ industrial catalysts, Science, 336 (2012) 893–897.
[92] R.G. González-Huerta, G. Ramos-Sánchez, P.B. Balbuena, Oxygen evolution in co-doped RuO_2 and IrO_2: experimental and theoretical insights to diminish electrolysis over-potential, J. Power Sources, 268 (2014) 69–76.
[93] L.D. Chen, M. Urushihara, K. Chan, J.K. Norskov, Electric field effects in electrochemical CO_2 reduction, ACS Catal., 6 (2016) 7133–7139.
[94] D.V. Vasilyev, P.J. Dyson, The role of organic promoters in the electroreduction of carbon dioxide, ACS Catal., 11 (2021) 1392–1405.
[95] C.C. Chang, M.S. Ku, Role of high-index facet Cu(711) surface in controlling the C_2 selectivity for CO_2 reduction reaction—a DFT study, J. Phys. Chem. C, 125 (2021) 10919–10925.
[96] W. Wang, X. Liu, J. Pérez-Ríos, Complex reaction network thermodynamic and kinetic autoconstruction based on Ab initio statistical mechanics: a case study of O_2 activation on Ag_4 clusters, J. Phys. Chem. A, 125 (2021) 5670–5680.
[97] S.G. Moore, D.R. Wheeler, Chemical potential perturbation: a method to predict chemical potentials in periodic molecular simulations, J. Chem. Phys., 134 (2011) 114514, doi: 10.1063/1.3561865.
[98] H. Lin, D.G. Truhlar, QM/MM: what have we learned, where are we, and where do we go from here?, Theor. Chem. Acc., 117 (2006) 185–199.
[99] K. Schwarz, R. Sundararaman, The electrochemical interface in first-principles calculations, Surf. Sci. Rep., 75 (2020) 100492, doi: 10.1016/j.surfrep.2020.100492.
[100] X. Shi, S. Back, T.M. Gill, S. Siahrostami, X.L. Zheng, Electrochemical synthesis of H_2O_2 by two-electron water oxidation reaction, Chem, 7 (2021) 38–63.